Composites Part B 97 (2016) 193–200

Contents lists available at ScienceDirect

Composites Part B

journal homepage: www.elsevier.com/locate/compositesb

Low-cycle fatigue behavior of 3d-printed PLA-based porous scaffolds

F.S. Senatov*, K.V. Niaza, A.A. Stepashkin, S.D. Kaloshkin

National University of Science and Technology "MISIS", 119049, Leninskiy pr. 4, Moscow, Russian Federation

ARTICLE INFO

Article history:
Received 23 January 2016
Received in revised form
26 March 2016
Accepted 26 April 2016
Available online 4 May 2016

Keywords:
A. Polymer-matrix composites (PMCs)
B. Fatigue
D. Mechanical testing
E. Lay-up (manual/automated)

ABSTRACT

In the present work PLA and PLA/15% wt. HA porous scaffolds for bone replacements with pre-modeled structure were obtained by 3D-printing by fused filament fabrication. The average pore size and porosity of the scaffolds were 700 μm and 30 vol. %, respectively. The modulus of elasticity, height of the samples, elastic deformation, accumulated energy and structural characteristics of 3D porous scaffolds were studied during the low-cycle tests. A decrease in the height, collapse of pores, delamination, bending and shear of the printed layers, growth and propagation of cracks during cyclic loading was observed. The introduction of dispersed HA particles reduced the rate of accumulation of defects. PLA/15%HA porous scaffolds with a larger crack resistance have the potential to be used as implants for trabecular bone replacement which are able to function under cyclic loading at a stress of 21 MPa for a long time without change.

1. Introduction

Polylactide (PLA) is a thermoplastic bioresorbable polymer which is of special interest in terms of medical application for bone reconstruction. Some works revealed the need to reinforce PLA matrix. As shown in a review of *Vieira* et al. [1] some attempts have been made to reinforce PLA mechanical properties through copolymers [2] and composites [3–5]. The most common way to increase its mechanical and osseointegration properties is to use calcium-phosphate particles like hydroxyapatite (HA) as a bioactive component [6–9]. Various authors have referred to the optimum content of HA particles in the bioresorbable matrix of 10–30%. As shown by *Sadat-Shojai* et al. [10] the concentration of 15% in PHB-matrix leads to formation of bone-like apatite and maximum mineralization; it also exhibits best cell response and improves cellular activity. Mechanical behavior of such PLA-based materials and scaffolds in compression was studied in Refs. [11–13].

The bioresorbable scaffold for bone defects replacement must be high-porous [14,15] with a typical pore size of 50–800 μm to provide an unhindered penetration of tissue cells and nutrients into implant [16,17]. Various technologies are using to create a porous structure in the bioresorbable polymers like PLA. These include the method of supercritical fluids [18] and blending with a porogen [19]. As shown in our previous work [20] PLA/HA porous scaffolds with porosity of 30 vol. % and the average pore size of 700 μm may be prepared also by 3D-printing based on the fused filament fabrication (FFF). 3D-printing is a rapidly developing method for producing bone tissue engineering scaffolds, which allows minimizing time of material processing at high temperatures to avoid thermodegradation of PLA. Biocompatibility of 3D-printed scaffolds and different aspects of interactions with cells have been demonstrated *in vitro* and *in vivo* in various studies [21–24].

A study of a fatigue behavior of porous composite material based on PLA used in loaded sites of the skeleton (maxillofacial, tubular bones, etc.) is of a great importance in view of the fact that under the cyclic load a large accumulation of defects occurs and an ultimate strength is reached much earlier than in static conditions and in some cases damage can occur at a stress below the yield strength of the material. According to *Misch* et al. the compressive strength of human mandible trabecular bone is in the range of 0.22–10.44 MPa [25]; maximum value for ultimate stress of human vertebral trabecular bone under compression is less than 4.5 MPa [26] and the mean value for bovine trabecular bone is 14.22 MPa [27], which fatigue strength is almost identical to that of the human [28]. Therefore, porous composite material based on PLA with yield strength over 21 MPa [20] may be used in implants for trabecular bone tissue replacements in different lightly loaded parts of skeleton.

Bone defect may be replaced with bone tissue during the resorption of the PLA scaffold. Fatigue cracks in the surrounding tissue under load can be repaired by the body during a certain

* Corresponding author.
E-mail address: Senatov@misis.ru (F.S. Senatov).

http://dx.doi.org/10.1016/j.compositesb.2016.04.067
1359-8368/

amount of time, and the fatigue strength at up to 10^5 cycles [28] represents the maximum stress range during a few days of normal activities [29]. At the same time resorption of PLA-based material by hydrolysis is a complex process taking place at different rates [30–32]. Therefore, behavior of PLA-based material at low-cycle loadings is of high interest. The works about a low-cycle fatigue behavior of such porous PLA-based structures are almost not found in the literature. In the present work a low-cycle fatigue behavior of 3D-printed PLA-based porous scaffolds for bone defects replacement was studied.

2. Material and methods

2.1. Preparation of test specimens

Polymer pellets of polylactide (PLA) (Mw = 60 000 g/mol, Aldrich) were used as a material for polymer-matrix. Hydroxyapatite (HA) powder with the average size of 1 micron produced by JSC "Polystom" (Russia) was used as the bioactive filler.

The method of obtaining the material and scaffolds is described in detail in the previous work [20]. Drying of initial PLA and HA was carried out at 80 °C for 4 h to prevent hydrolysis and oxidative degradation. Mixing of PLA and 15 wt. % HA powder was carried out in a screw extruder HAAKE MiniLab II Micro Compounder (Thermo Fisher Scientific) for 15 min at 30 rev/min at a temperature of 180 °C. Filaments of PLA/HA composites 1.7 ± 0.2 mm in diameter were obtained in this way.

The structure of a 3D scaffold was modeled using SolidWorks 2015 software (SolidWorks Corporation, Santa Monica, CA, USA). Netfabb Basic 5.2 software was used to analyze STL-files. The modeled pore size was 800 μm. All pores were interconnected. Porosity of the scaffolds was at a level of 30 vol. %.

3D-printing of porous scaffolds was performed using CubePro Trio (3D Systems, Inc.) by FFF at a nozzle temperature of 180 °C and 210 °C for PLA and PLA/HA scaffolds, respectively. A nozzle with a diameter of 350 μm was used. The thickness of a single layer was 200 μm. Printing rate was 30 mm/s. Porous samples were treated for 30 min in an ultrasonic bath to remove residual surface particles and ledges after 3D-printing. Rectangular samples of scaffolds were obtained (Fig. 1).

2.2. Structure characterization

Studies of 3D porous scaffolds before and after cyclic loading were conducted by scanning electron microscopy (SEM). SEM was performed with Hitachi TM-1000 (accelerating voltage 5 kV). To investigate non-conductive polymer samples, the surface of the samples was covered with a layer of platinum (10–20 nm) by Auto Fine Coater JFC-1600 (Jeol, USA).

2.3. Study of mechanical properties

Mechanical testing was performed in a universal testing machine Zwick/Roell Z 020, (Zwick GmbH & Co. KG, Germany) using rectangular samples of scaffolds with the cross-sectional dimensions of 24 mm × 12.5 mm for compression tests under cyclic loading and in static conditions (ASTM D695). The ultimate stresses in static conditions for PLA and PLA/HA samples were 30 MPa and 54 MPa, respectively. Low-cycle compressive fatigue tests were performed at 18, 21, 24, 27, 30, 33 MPa. Stress rates are shown in Table 1. Three samples were tested for each strain rate. Low-cycle fatigue tests (lifetime more than 1000 cycles) were performed at a frequency of 0.2 Hz in a "soft"-cycle mode with stress control. The deformation was measured by the deformation sensor. The coefficient of the loop symmetry was calculated:

$$R = \frac{\sigma_{min}}{\sigma_{max}}, \quad (1)$$

where σ_{min} = 2.8 MPa, σ_{max} = 21 MPa, R = 0.13.

Table 1
Stress rates during low-cycle compressive fatigue tests for PLA and PLA/HA samples.

Stress, MPa	Stress rate		Stress considering the cross-section of the samples, MPa	
	PLA	PLA/HA	PLA	PLA/HA
18	0.60σ	–	21.8	–
21	0.70σ	0.39σ	25.4	27.5
24	0.80σ	0.44σ	29	31.4
27	0.90σ	0.50σ	32.7	35.4
30	–	0.55σ	–	39.3
33	–	0.61σ	–	43.2

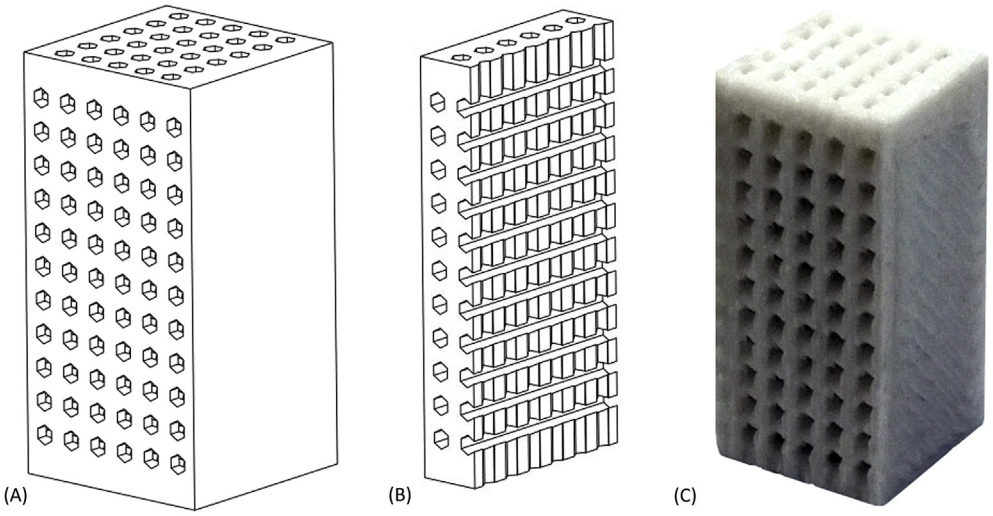

Fig. 1. Computer model (A), cut-away model (B) and PLA/HA scaffold obtained by 3D-printing (C).

3. Results and discussion

3.1. Low-cycle fatigue tests

The initial level of the cyclic loading was chosen such that the first stage was in the region of linear deformation of the material (within the region 2, Fig. 2A,B) and the second stage was lower than the yield point (the transition to the region 3, Fig. 2A,B). Thereby, the first 1000 cycles for PLA and PLA/HA porous scaffolds were performed at 18 and 21 MPa, respectively.

An accumulation of defects, such as micro-delamination at the interfaces between layers, micro cracks in the layers, and an accumulation of local plastic deformation was occurred during the cyclic loading of the material.

The shift of the hysteresis loop (Fig. 2C) allows evaluating the value of an accumulated deformation to the corresponding cycle [33,34]. The change in the width and area of the hysteresis loop allows evaluating the value of a reversible deformation and energy which was dissipated during cyclic loading [33,34]. The energy dissipated in the sample within the cycle was spent on the formation of defects and was released as heat [33–35].

A decrease in the total height of the sample, a change in the tangent modulus, a value of energy dissipated in the material and kinetics of an accumulation of deformation were measured during the cyclic loading.

The complex state of stress was formed under the influence of cyclic loads in the material. Predominantly compressive stresses acted in the vertical direction (in rod-like segments of scaffold) and mainly tensile stresses acted in the horizontal layers. Residual tensile stresses without loading tend to return the specimen to its original state, which made a major contribution to the restoration of height.

The "stress – deformation" curve at the initial stage is typical for porous materials (Fig. 2a, region 1). Collapse of micropores within the printed layers and local deformations of the scaffold elements occurred with an increase of loading. Formation of microcracks in the bending layers occurred with the development of fatigue process and further led to the main crack propagation and destruction of the scaffold (Fig. 3).

Changing of the shape of the sample, primarily the height (Fig. 4), depends on the level of maximum stress at a cycle. At the maximum stress less the yield strength of the material (within the region 2, Fig. 2a) the main changes in height occurred within the first 50–60 cycles of loading, after which the rate of height changing was reduced. The height of the samples stabilized up to 400–500 cycles and remained substantially unchanged. This corresponds to a stress of 18 MPa in the case of PLA (Fig. 4a) and 21 MPa in the case of PLA/HA (Fig. 4b). It can be assumed that the scaffold after a pre-strain may further operate a long time without a failure at such level of stress.

Mechanical behavior of the samples began to change with an increase in maximum stress at a cycle to a value close to the yield strength of the material under static conditions: level 2, corresponding to 24 MPa for PLA (Fig. 4a) and 27 MPa for PLA/HA (Fig. 4b). Initially, the height changing of the samples proceeded similarly to the level 1, but the rate of the height changing began to increase after 800–900 cycles, most notably for pure PLA (Fig. 4a). Filling the PLA matrix with dispersed HA particles reduced the fluidity of the material and had a positive effect on the stability of the sample (Fig. 4b).

The role of the fluidity processes increased with increasing the maximum stress at a cycle. Stabilization of the height of the sample at some equilibrium level did not occur, as was observed at lower loads. At the last stage at a maximum stress of 27 MPa for pure PLA

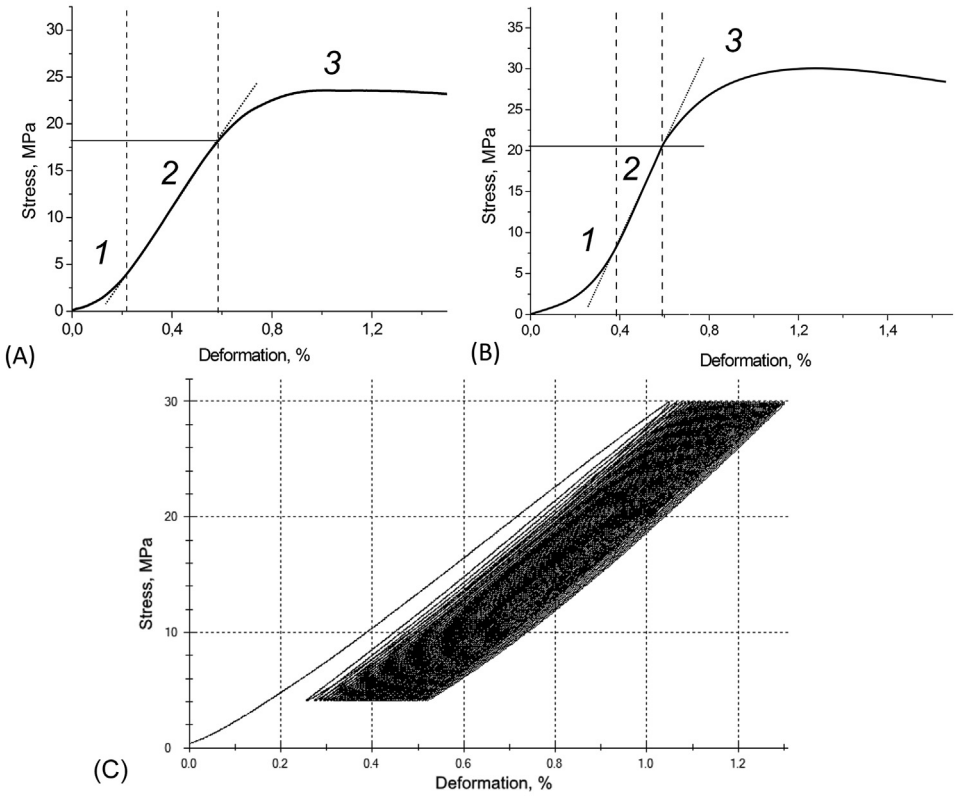

Fig. 2. Example of a "stress - deformation" curve in a static condition for PLA (A) and PLA/HA composite (B) and low-cycle test (C). 1 – region of non-linear deformation; 2 – linear region; 3 – yield region.

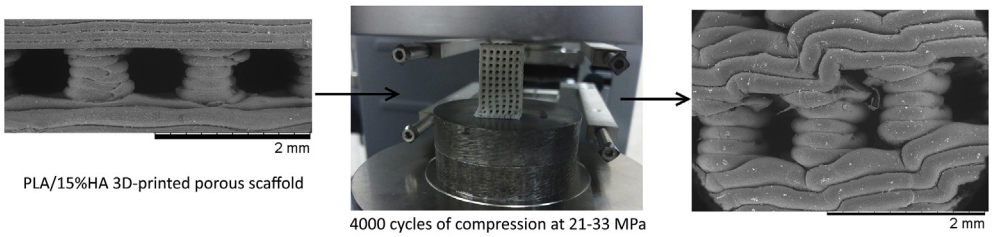

Fig. 3. Microstructure of PLA-based porous scaffold before and after cyclic loading.

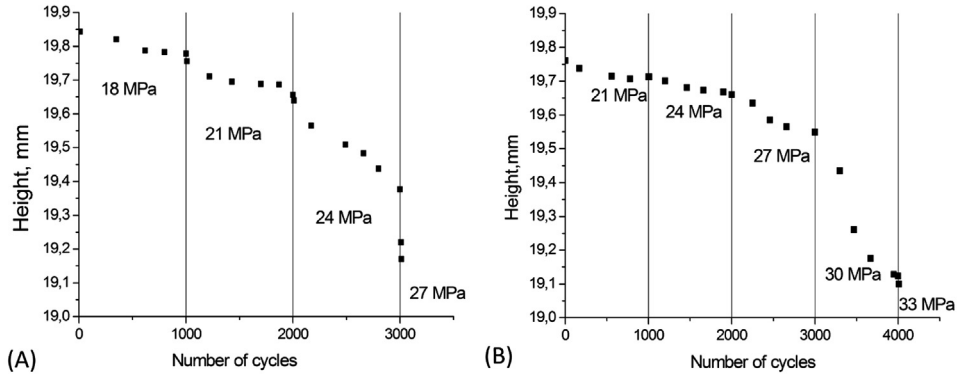

Fig. 4. Change in height of PLA (A) and PLA/HA (B) porous scaffold specimens at different loadings.

and 33 MPa for the PLA/HA composite the destruction occurred in the range of 20–30 cycles.

Estimation of the dynamics of height changing of the sample allows estimating the operating life of the scaffold at different stress levels.

A break in the cyclic loading led to a partial recovery of the shape and size of the samples, due to the processes of relaxation of stresses in the material. Fig. 5 shows the change in the height of the samples during cyclic loading. When the height changing began to increase and the change was over 50–100 μm then the sample was removed from the test and a break in loading occurred. This corresponds to the breakpoint in Fig. 5. Behavior of the presented curves (Fig. 5) was determined by measurements for individual PLA and PLA/HA samples. A break in the loading led to a restoration of the height of the samples by 20–40% (line 1 in Fig. 5). Curves of the height changing were back to the standard behavior (line 2 in Fig. 5) within 200 cycles after the continuation of the tests.

Change in the elastic modulus (Fig. 6) on the one hand was due to the collapse of the micropores, the denser structure, and on the other hand due to the accumulation of microdamages and deformations. The similar situation was discussed in the work of *Hoque* et al. [23] in the case of PEG-PCL-PLA 3D-printed scaffolds. Therefore, in the early stages of loading, there was some increase in the elastic modulus. The rate of accumulation of defects increased with increasing of the maximum stress at a cycle, which led to a lower modulus values.

Change in the elastic modulus behavior was observed at stresses of more than 21 MPa for both PLA and PLA/HA scaffolds, when the process of accumulation of damages and deformations in the material brought to the reduction of the modulus. The rate of decrease in an elastic modulus for PLA/HA composite was lower than for pure PLA. The intensive destruction of the structure and the modulus reduction was observed at a certain critical value of the stress (27 MPa for PLA and 32 MPa for PLA/HA), beginning with the first cycle. In contrast, in the work of *Del Vecchio* et al. [36], studied the behavior of polyester under cyclic compression, a weak effect strain rate during cyclic loadings on the modulus of elasticity was found, but there was a significant change in a maximum stress and

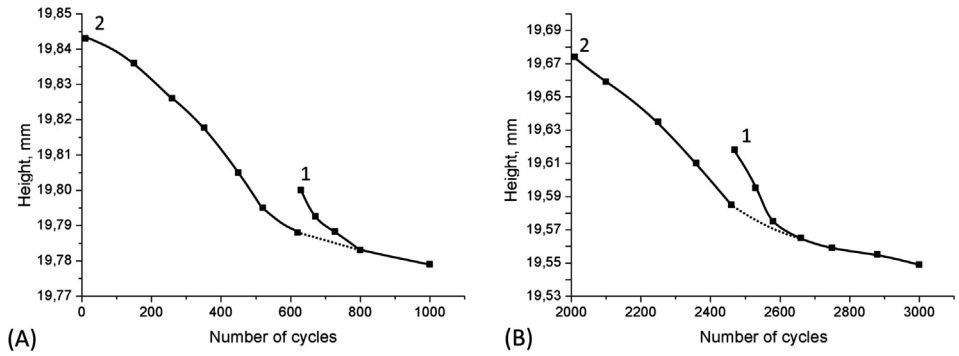

Fig. 5. Change in height of PLA (A) and PLA/HA (B) porous scaffold under cyclic loading with (1) and without relaxation (2).

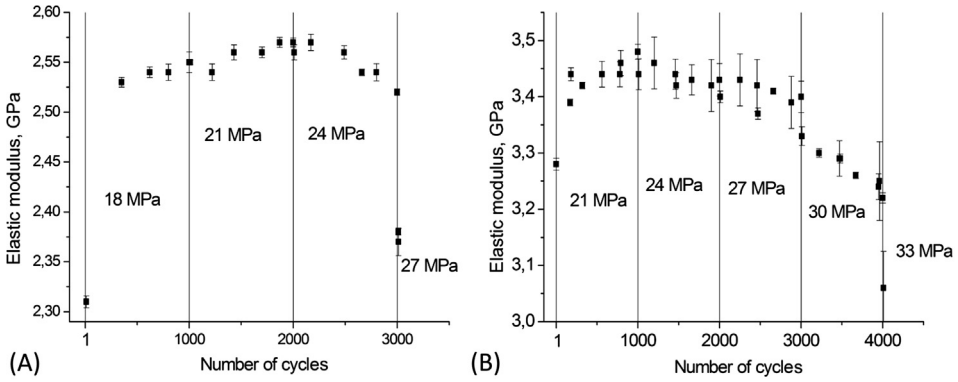

Fig. 6. Elastic modulus of PLA (A) and PLA/HA (B) porous scaffolds in compression at different loadings.

proportional stress. But the similar behavior was observed by *Michel* et al. [37] in case of bovine trabecular bone when modulus slightly increased for low levels of applied cyclic stress and the fatigue behavior began after plastic deformation initiation, followed by accumulation of deformations and modulus reduction [37].

The deformation behavior of the material during cyclic loading is shown in Fig. 7. Within the first 40–100 loading cycles at each of the stages there was a considerable increase in the value of the accumulated deformation (Fig. 7, curve A), whereupon the processes of accumulation of deformation decreased and reached a constant level, depending on the value of the maximum stress at a cycle. The width of the hysteresis loop in the process of loading decreased, i.e. material showed a tendency to a cyclic hardening.

The elastic deformation within the cycle did not change (Fig. 7, curve B). The hysteresis loop was increased after 3000 and 4000 cycles for PLA and PLA/HA samples of porous scaffolds, respectively, and the material was entering a stage of destruction.

Total deformation (Fig. 7, curve C) increased with increasing of a stress at a cycle. As can be seen from the data the material destruction occurred after 3000 and 4000 cycles for samples of porous scaffolds PLA and PLA/HA, respectively, at the values close to the yield strength of the material under static conditions (Fig. 7, line D). This allows using the deformation criterion for assessing the operating life of the scaffold for a given level of a maximum stress. PLA and PLA/HA porous scaffolds exhibited a similar mechanical behavior. The only difference was in the value of stresses and deformations. It should also be noted that PLA/HA scaffold accumulated defects more slowly than PLA scaffold, so there was a less accumulated energy for the same number of cycles.

The energy dissipated in the material in one cycle consisted of the loss of heat and the formation of defects. An area of the hysteresis loop was reduced during the loading. It tends to be a cyclic hardening of the material. There was an increase of the accumulated energy for PLA and PLA/HA with increasing of a stress during cyclic tests, as shown in Fig. 8.

3.2. Structure of PLA and PLA/HA porous scaffolds after cyclic loading

PLA/HA porous scaffolds demonstrated a larger crack resistance in the initial stages of cyclic loading. HA particles inhibited the growth of cracks [20] during cyclic loadings. The same behavior when ceramic nanoparticles retarded the crack formation was observed in the case of PLA/nanoclay samples in the fatigue studies performed by *Averett* et al. [38] at frequencies of 3 and 30 Hz.

Destruction of the material took place by the shift mechanism. The crack was growing at 45° to the direction of applied load. Typically, the destruction started at a point adjacent to the support (lower left corner of the sample in Figs. 9 and 10).

The structure of the loaded porous PLA and PLA/HA constructions was similar to the structure of porous PEG-PCL-PLA 3D-printed scaffolds which were formed in the work of *Hoque* et al. [23] by 0/90° layers deposition with formation of "column" structure. The same was observed for other compositions: PLA/PEG/CaP-glass [24,39] and PLA-TCP porous scaffolds [40]. *Hoque* et al. showed that such scaffold structure appeared as the most resistant to compression.

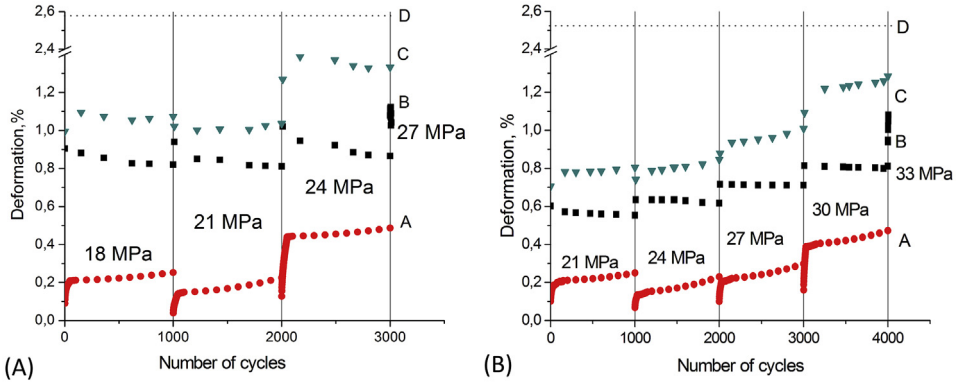

Fig. 7. Deformation of PLA (A) and PLA/HA (B) porous scaffolds at different loadings. A – accumulated deformation, B – elastic deformation, C – total deformation, D – deformation at destruction under static conditions.

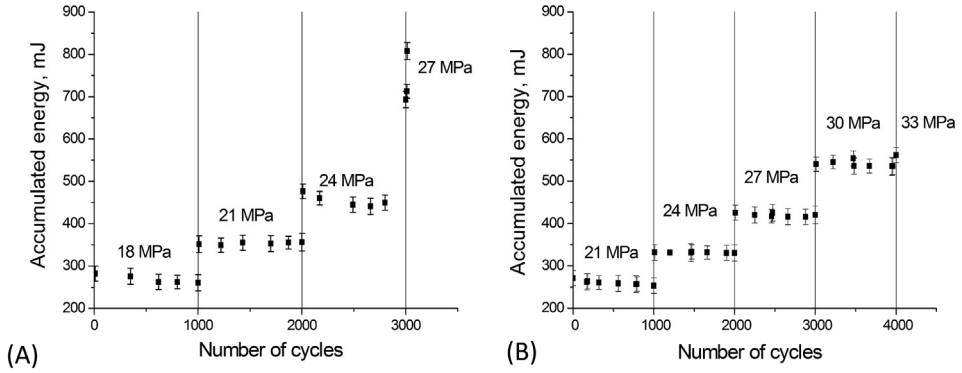

Fig. 8. Accumulated energy of PLA (A) and PLA/HA (B) porous scaffolds at different loadings.

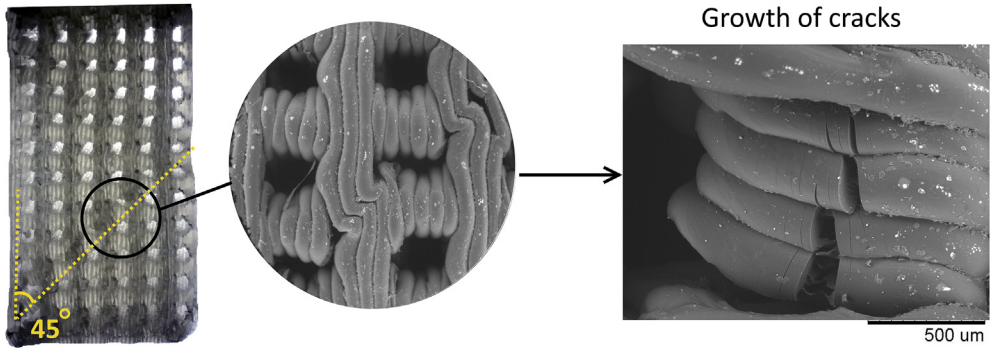

Fig. 9. Structure of PLA porous scaffold after cyclic loading (4000 cycles).

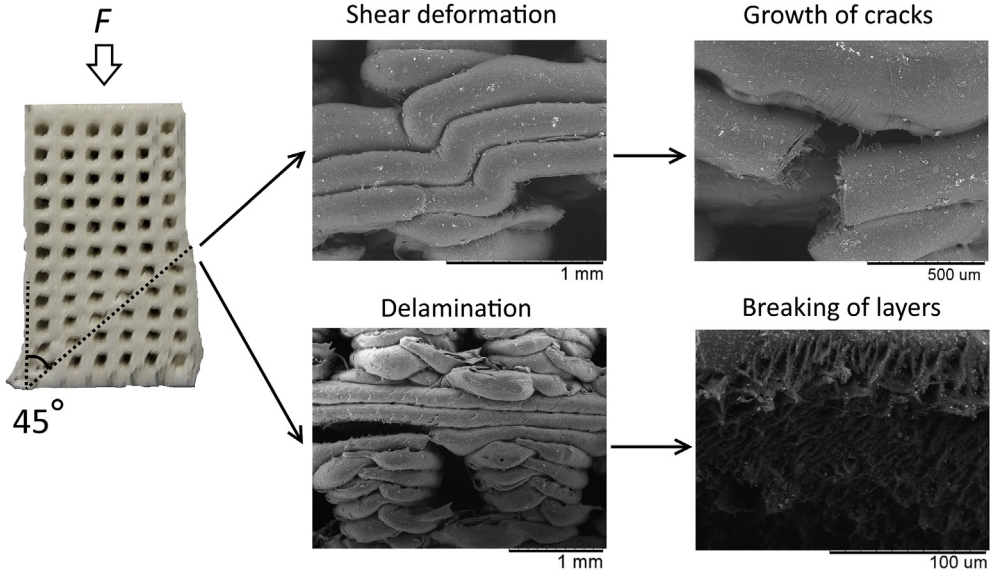

Fig. 10. Structure of PLA/HA porous scaffold after cyclic loading (4000 cycles).

Fractographical studies with SEM showed that the initial lesions occurred at the interface between the printed layers. Destruction of the interfaces led to a shift of the layers relative to each other and a formation of wrinkles under the influence of shear stresses (Figs. 9 and 10). Formation and growth of the microcracks occurred in the bends of the layers, the development of which further led to the appearance and growth of the main crack. However, it should be noted that PLA/HA composite layers firmly adhered to each other by welding during 3D-printing, as shown by the areas of plastic deformation of PLA matrix in the micrograph of the fracture surface (breaking of layers in Fig. 10). The similar situation was observed by *Jiang* et al. [41], when neat PLA tested under uniaxial tension showed smooth fracture surfaces and PLA/$CaCO_3$ composites showed more yielding fracture surfaces because of larger plastic

deformation.

Therefore, the data obtained demonstrate that PLA/15%HA porous scaffolds with a larger crack resistance obtained by 3D-printing have the potential to be used as implants for bone replacement which are able to function under cyclic loading at a stress of 21 MPa for a long time without change. Quantitative evaluation of such time is also important, since the behavior of a material under load is very different from the behavior of natural bone. PLA and PLA/HA scaffolds demonstrated fatigue behavior under low-cycle loading. However, in case of bone tissue a creep damage usually takes place as shown by Carter & Caler [42,43]. This may be an important difference between natural and synthetic material under low-cycle repeated loadings. Therefore, quantitative evaluation is an important and challenging problem for future studies.

4. Conclusions

PLA-based porous scaffolds for bone implants with the average pore size of 700 μm and porosity of 30 vol. % were prepared by 3D-printing based on fused filament fabrication. All pores were interconnected. Scaffolds exhibited hysteresis in low-cycle fatigue tests, which means the formation of defects and the accumulation of plastic deformation.

A decrease in the height of the samples, collapse of pores, delamination, bending and shear of the printed layers, growth and propagation of cracks during cyclic loading was observed. Bending of the printed layers led to the destruction of the scaffolds material. The height change was stabilized with a load of 18 MPa in the case of PLA and 21 MPa in the case of PLA/HA scaffolds. The possibility of functioning of the porous scaffold at such stress for a long time without change can be assumed.

The rate of defects formation increased with the increase of stress. This led to increased pliability of the porous structure and a reduction in modulus of elasticity. The rate of accumulation of defects for PLA porous scaffolds was higher. The introduction of dispersed HA particles reduced the rate of accumulation of defects. PLA/HA porous scaffolds demonstrated a larger crack resistance in the initial stages of cyclic loading. HA particles inhibited the growth of cracks during cyclic loadings. The area of the hysteresis was reduced during the loading. A cyclic hardening of the material was observed. There was an increase of the accumulated energy for PLA and PLA/HA with an increase in a stress during the cyclic tests.

The data obtained demonstrate that PLA/15%HA porous scaffolds obtained by 3D-printing have the potential to be used as implants for trabecular bone replacement which are able to function under cyclic loading.

Acknowledgments

This work was supported by the Federal Targeted Program “Research and development in priority directions of development of scientific technological complex of Russia in 2014–2020”, with the funding from the Ministry of Education and Science of Russian Federation: agreement 14.575.21.0088, 21 October 2014, RFMEFI57514X0088.

References

[1] Vieira AC, Guedes RM, Marques AT. Development of ligament tissue biodegradable devices: a review. J Biomech 2009;42(15):2421–30.
[2] Guarino V, Causa F, Taddei P, di Foggia M, Ciapetti G, Martini D. Polylactic acid fibre-reinforced polycaprolactone scaffolds for bone tissue engineering. Biomaterials 2008;29(27):3662–70.
[3] McCarthy SP, Ranganthan A, Ma W. Advances in properties and biodegradability of co-continuous, immicisible, biodegradable, polymer blends. Macromol Symp 1999;144(1):63–72.
[4] Wong S, Shanks RA, Hodzic A. Mechanical behavior and fracture toughness of poly(L-lactic acid)-natural fiber composites modified with hyperbranched polymers. Macromol Mater Eng 2004;289(5):447–56.
[5] Yuan Y, Ruckenstein E. Polyurethane toughened polylactide. Polym Bull 1998;40(4):485–90.
[6] Persson M, Lorite GS, Kokkonen HE, Cho S-W, Lehenkari PP, Skrifvars M, et al. Effect of bioactive extruded PLA/HA composite films on focal adhesion formation of preosteoblastic cells. Coll Surf B Biointerfaces 2014;121:409–16.
[7] Zheng X, Zhou S, Li X, Wenig J. Shape memory properties of poly(D,L-lactide)/hydroxyapatite composites. Biomaterials 2006;27:4288–95.
[8] Kutikov A, Song J. An amphiphilic degradable polymer/hydroxyapatite composite with enhanced handling characteristics promotes osteogenic gene expression in bone marrow stromal cells. Acta Biomater 2013;9(9):8354–64.
[9] Hong Z, Zhang P, He C, Qiu X, Liu A, Chen L, et al. Nano-composite of poly(L-lactide) and surface grafted hydroxyapatite: mechanical properties and biocompatibility. Biomaterials 2005;26:6296–304.
[10] Sadat-Shojai M, Khorasani M-T, Jamshidi A, Irani S. Nano-hydroxyapatite reinforced polyhydroxybutyrate composites: a comprehensive study on the structural and in vitro biological properties. Mater Sci Eng C 2013;33(5):2776–87.
[11] Nie L, Chen D, Fu J, Yang S, Hou R, Suo J. Macroporous biphasic calcium phosphate scaffolds reinforced by poly-L-lactic acid/hydroxyapatite nanocomposite coatings for bone regeneration. Biochem Eng J 2015;98:29–37.
[12] Felfel RM, Ahmed I, Parsons AJ, Walker GS, Rudd CD. In vitro degradation, flexural, compressive and shear properties of fully bioresorbable composite rods. J Mech Behav Biomed Mater 2011;4:1462–72.
[13] Rakovsky A, Gotman I, Rabkin E, Gutmanas EY. β-TCP–polylactide composite scaffolds with high strength and enhanced permeability prepared by a modified salt leaching method. J Mech Behav Biomed Mater 2014;32:89–98.
[14] Ma PX. Scaffold for tissue engineering. Mater Today 2004;7(5):30–40.
[15] Guarino V, Ambrosio L. The synergic effect of polylactide fiber and calcium phosphate particle reinforcement in poly e-caprolactone-based composite scaffolds. Acta Biomater 2008;4:1778–87.
[16] Hollister SJ, Lin CY, Saito E, Lin CY, Schek RD, Taboas JM, et al. Engineering craniofacial scaffolds. Orthod Craniofac Res 2005;8(3):162–73.
[17] Karageorgiou V, Kaplan D. Porosity of 3D biomaterial scaffolds and osteogenesis. Biomaterials 2005;26(27):5474–91.
[18] Keshtkar M, Nofar M, Park CB, Carreau PJ. Extruded PLA/clay nanocomposite foams blown with supercritical CO2. Polymer 2014;55:4077–90.
[19] Nam YS, Yoon JJ, Park TG. A novel fabrication method of macroporous biodegradable polymer scaffolds using gas foaming salt as a porogen additive. J Biomed Mater Res 2000;53:1–7.
[20] Senatov FS, Niaza KV, MYu Zadorozhnyy, Maksimkin AV, Kaloshkin SD, Estrin YZ. Mechanical properties and shape memory effect of 3D-printed PLA-based porous scaffolds. J Mech Behav Biomed Mater 2016;57:139–48.
[21] Bose S, Vahabzadeh S, Bandyopadhyay A. Bone tissue engineering using 3D printing. Mater Today 2013;16(12):496–504.
[22] Scaffaro R, Re GL, Rigogliuso S, Ghersi G. 3D polylactide-based scaffolds for studying human hepatocarcinoma processes in vitro. Sci Technol Adv Mater 2012;13:045003.
[23] Hoque ME, Hutmacher DW, Feng W, Li S, Huang MH, Vert M, et al. Fabrication using a rapid prototyping system and in vitro characterization of PEG-PCL-PLA scaffolds for tissue engineering. J Biomater Sci Polym Edn 2005;16(12):1595–610.
[24] Serra T, Planell YA, Navarro M. High-resolution PLA-based composite scaffolds via 3-D printing technology. Acta Biomater 2013;9:5521–30.
[25] Misch CE, Qu Z, Bidez MW. Mechanical properties of trabecular bone in the human mandible: implications for dental implant treatment planning and surgical placement. J Oral Maxillofac Surg 1999;57(6):700–6.
[26] Kopperdahl DL, Keaveny TM. Yield strain behavior of trabecular bone. J Biomech 1998;31:601–8.
[27] Fatihhi SJ, Rabiatul AAR, Harun MN, Kadir MRA, Kamarul T, Syahrom A. Effect of torsional loading on compressive fatigue behaviour of trabecular bone. J Mech Behav Biomed Mater 2016;54:21–32.
[28] Taylor D. Scaling effects in the fatigue strength of bones from different animals. J Theor Biol 2000;206(2):299–306.
[29] Whalen RT, Carter DR, Steele CR. Influence of physical activity on the regulation of bone density. J Biomech 1988;21:825–37.
[30] Russias J, Saiz E, Nalla RK, Gryn K, Ritchie RO, Tomsia AP. Fabrication and mechanical properties of PLA/HA composites: a study of in vitro degradation. Mater Sci Eng C 2006;26:1289–95.
[31] Roshan-Ghias A, Lambers FM, Gholam-Rezaee M, Müller R, Pioletti DP. In vivo loading increases mechanical properties of scaffold by affecting bone formation and bone resorption rates. Bone 2011;49:1357–64.
[32] Montjovent MO, Mark S, Mathieu L, Scaletta C, Scherberich A, Delabarde C, et al. Human fetal bone cells associated with ceramic reinforced PLA scaffolds for tissue engineering. Bone 2008;42:554–64.
[33] Shtremel MA. Destruction. The destruction of material Moscow. MISIS Publishing. House; 2014 [in Russian].
[34] Rie KT. Low cycle fatigue and elasto-plastic behaviour of materials. Netherlands: Springer; 1987.
[35] Schijve J. Fatigue of structures and materials. Netherlands: Springer; 2009.
[36] Del Vecchio FJC, Reis JML, da Costa Mattos HS. Elasto-viscoplastic behaviour of polyester polymer mortars under monotonic and cyclic compression. Polym

Test 2014;35:62–72.
[37] Michel MC, Guo XD, Gibson LJ, McMahon TA, Hayes WC. Compressive fatigue behavior of bovine trabecular bone. J Biomech 1993;26:453–63.
[38] Averett RD, Realff ML, Jacob K, Cakmak M, Yalcin B. The mechanical behavior of poly(lactic acid) unreinforced and nanocomposite films subjected to monotonic and fatigue loading conditions. J Compos Mater 2011;45(26): 2717–26.
[39] Serra T, Ortiz-Hernandez M, Engel E, Planell JA, Navarro M. Relevance of PEG in PLA-based blends for tissue engineering 3D-printed scaffolds. Mater Sci Eng C 2014;38:55–62.
[40] Martinez-Vazquez FJ, Perera FH, Miranda P, Pajares A, Guiberteau F. Improving the compressive strength of bioceramic robocast scaffolds by polymer infiltration. Acta Biomater 2010;6:4361–8.
[41] Jiang L, Zhang J, Wolcott MP. Comparison of polylactide/nano-sized calcium carbonate and poly- lactide/montmorillonite composites: reinforcing effects and toughening mechanisms. Polymer 2007;48(26):7632–44.
[42] Carter DR, Caler WE. A cumulative damage model for bone fracture. J Orthop Res 1985;3(1):84–90.
[43] Carter DR, Hayes WC. Compact bone fatigue damage: a microscopic examination. Clin Orthop 1977;127:265–74.